J. Lundén, V. Koivunen, A. Huttunen and H. V. Poor, "Collaborative cyclostationary spectrum sensing for cognitive radio systems," *IEEE Transactions on Signal Processing*, vol. 57, no. 11, November 2009.

Collaborative Cyclostationary Spectrum Sensing for Cognitive Radio Systems

Jarmo Lundén, *Student Member, IEEE*, Visa Koivunen, *Senior Member, IEEE*, Anu Huttunen, and H. Vincent Poor, *Fellow, IEEE*

***Abstract*—This paper proposes an energy efficient collaborative cyclostationary spectrum sensing approach for cognitive radio systems. An existing statistical hypothesis test for the presence of cyclostationarity is extended to multiple cyclic frequencies and its asymptotic distributions are established. Collaborative test statistics are proposed for the fusion of local test statistics of the secondary users, and a censoring technique in which only informative test statistics are transmitted to the fusion center (FC) during the collaborative detection is further proposed for improving energy efficiency in mobile applications. Moreover, a technique for numerical approximation of the asymptotic distribution of the censored FC test statistic is proposed. The proposed tests are nonparametric in the sense that no assumptions on data or noise distributions are required. In addition, the tests allow dichotomizing between the desired signal and interference. Simulation experiments are provided that show the benefits of the proposed cyclostationary approach compared to energy detection, the importance of collaboration among spatially displaced secondary users for overcoming shadowing and fading effects, as well as the reliable performance of the proposed algorithms even in very low signal-to-noise ratio (SNR) regimes and under strict communication rate constraints for collaboration overhead.**

***Index Terms*—Censoring, cognitive radio, collaborative spectrum sensing, cyclostationary detection, energy efficient detection.**

I. Introduction

WIRELESS communication systems rely on the use of scarce resources, most notably the radio frequency spectrum. The dramatic increases in the number of wireless subscribers, the advent of new applications and the continuous demand for higher data rates call for flexible and efficient use of the frequency spectrum. Cognitive radios have been proposed as a technology for dynamic spectrum allocation [1]–[3]. Cognitive radios sense the radio spectrum in order to find temporal and spatial spectral opportunities and adjust their transceiver parameters and operation mode accordingly. Spectrum sensing has to be done reliably in the face of propagation effects such as shadowing and fading. Moreover, the level of interference caused to the primary (legacy) users of the spectrum must be maintained at a tolerable level.

Different approaches for spectrum sensing for cognitive radio applications have been proposed, e.g., [2] and [4]–[8]. The commonly considered approaches are based on power spectrum estimation, energy detection, and cyclostationary feature detection. Power spectrum estimation may not work reliably in the low signal-to-noise ratio (SNR) regime. Energy detection, on the other hand, is subject to uncertainty in noise and interference statistics. In addition, neither power spectrum estimation nor energy detection are able to distinguish among the primary user signals, secondary user signals, or interference. Cyclostationary detection allows classifying co-existing signals exhibiting cyclostationarity at different cyclic frequencies, relaxing assumptions on noise statistics and has reliable performance even in the very low SNR regime.

In this paper we propose an extension of the time-domain Neyman–Pearson (NP) type test for the presence of second-order cyclostationarity of [7] to simultaneous use of multiple cyclic frequencies. Moreover, the maximum and sum of the cyclic autocorrelation test statistics over the cyclic frequencies of interest are considered. The proposed multicycle detectors are based on the classical cyclic autocorrelation estimator and its asymptotic properties. The method is nonparametric in the sense that no assumptions on the noise and data distribution are required. The only essential assumption required is the knowledge of at least one cyclic frequency of the primary user's signal. Under the null hypothesis the asymptotic distribution established provides an accurate approximation for all the signal lengths of interest. The NP formulation provides a rigorous way of limiting the false alarm rate to an acceptable level, which is necessary for allowing the cognitive radio to access the available spectrum on a regular basis, independently of the underlying noise and interference statistics. Finally, the method is applicable for detecting almost cyclostationary signals where the cyclic period may not be an integer number. See [9] for a discussion of the benefits and limitations of the method of [7] among others for cyclic period estimation.

In order to guarantee that the interference caused to the primary users is below an allowed level, the secondary users need

Manuscript received May 26, 2008; accepted May 15, 2009. First published June 12, 2009; current version published October 14, 2009. The associate editor coordinating the review of this manuscript and approving it for publication was Prof. Yonina C. Eldar. J. Lundén's work was supported by GETA graduate school, Finnish Defence Forces Technical Research Centre, and Nokia Foundation. The funding for V. Koivunen's sabbatical term at Princeton University was provided by the Academy of Finland. H. Vincent Poor's work was supported by the U.S. National Science Foundation under Grants ANI-03-38807 and CNS-06-25637. Some preliminary results of this work were presented in part at the Second International Conference on Cognitive Radio Oriented Wireless Networks and Communications, Orlando, FL, July 31–August 3, 2007 and the Forty-First Asilomar Conference on Signals, Systems, and Computers, Pacific Grove, CA, November 4–7, 2007.

J. Lundén and V. Koivunen are with the Department of Signal Processing and Acoustics, SMARAD CoE, Helsinki University of Technology, FI-02015 TKK, Finland(e-mail: jrlunden@wooster.hut.fi; visa@wooster.hut.fi).

A. Huttunen is with Nokia, Finland (e-mail: anu.huttunen@nokia.com).

H. V. Poor is with the Department of Electrical Engineering, Princeton University, Princeton, NJ 08544 USA (e-mail: poor@princeton.edu).

Color versions of one or more of the figures in this paper are available online at http://ieeexplore.ieee.org.

Digital Object Identifier 10.1109/TSP.2009.2025152

to perform spectrum sensing reliably in the face of severe shadowing and fading effects. Overcoming these effects without excessively long detection times requires collaboration among secondary users. Collaboration among spatially displaced secondary users allows mitigation of shadowing and fading effects. However, collaborative detection schemes may lead to substantial overhead traffic generated by the transmission of the observed data, local test statistics or decisions to the FC. The amount of data transmitted should be minimized especially in mobile, battery operated terminals due to stringent battery life constraints or when the control channel has low capacity.

We further extend the single user multicycle tests proposed in this paper to accommodate collaboration among the secondary users. The global decisions are made by combining the local test statistics in a dedicated FC or in an ad hoc manner by the secondary users. The proposed tests allow simple decision making and threshold selection at the FC. Furthermore, in order to reduce the amount of data transmitted during collaborative detection, we propose a censoring scheme in which only informative test statistics are sent to the FC. In addition to the test statistics, the only parameters transmitted to the FC during the censoring process are the communication rate constraints of the individual secondary users. We propose a comprehensive way of determining the censoring and detection thresholds given the communication and false alarm rate constraints. The proposed method is easy to implement in practice and causes only minimal performance loss compared to the uncensored approach even under very strict communication rate constraints.

Multicycle detection has received considerable amount of attention in the past. Optimum and locally optimum multicycle detectors have been proposed in [10] and [11]. However, these detectors cannot be implemented without the knowledge of the signal phase. Moreover, they require an explicit assumption on the noise distribution. Many suboptimum multicycle detectors with different requirements and properties have been proposed in the literature. A comprehensive bibliography on cyclostationary detection and cyclostationarity in general is provided in [12].

Many of the collaborative detection techniques stem from distributed detection theory; see e.g., [13] and [14]. Collaborative spectrum sensing methods based on energy detection have been proposed, e.g., in [5] and [6]. In [15] and [16] cooperation strategies using amplify-and-forward (AF) protocol have been proposed. Cyclostationarity based collaborative detection has been previously considered in [17] where binary decisions of the secondary users using cyclic detectors are combined. Optimal test thresholds at the FC and the secondary users are determined using an iterative algorithm. However, due to the iterative nature of the algorithm, multiple expensive transmissions between the FC and the secondary users are required.

Censoring techniques have been previously proposed for energy efficient sensor networks in [18], [19], and in [20] where the energy efficiency is further improved by ordering the node transmissions. Collaborative spectrum sensing with censoring for cognitive radios has been considered in [21] where energy detection is combined with censoring and transmission of binary decisions. In this paper censoring is combined with cyclostationary detection and secondary users transmit their local test statistics instead of binary decisions. Hence, the thresholds for detection and censoring must be determined differently.

The contributions of the paper are as follows. The paper proposes a powerful energy efficient approach for spectrum sensing that combines cyclostationary detection and user collaboration with censoring. Single user multicycle tests for detecting the primary user signals are proposed. Reduced complexity versions of the multicycle detectors are proposed as well. The proposed multicycle detectors are extended to accommodate collaboration among multiple secondary users. A censoring scheme reducing the amount of data transmitted in collaborative detection of secondary users is proposed. The asymptotic distributions of the test statistics under the null hypothesis are established. The established asymptotic distributions are based on the asymptotics of the cyclic correlation estimators. Hence, the proposed tests are nonparametric in the sense that no assumptions on data or noise distributions are required. Simulation experiments showing the benefits of the proposed cyclostationary approach compared to energy detection, the importance of collaboration among spatially displaced secondary users for overcoming shadowing and fading effects, as well as the reliable performance of the proposed algorithms even in very low SNR regimes and under strict communication rate constraints are provided.

The paper is organized as follows. Novel single user multicycle detectors are proposed in Section II. In particular, the problem is formulated as an hypothesis testing problem, and corresponding generalized likelihood ratio tests (GLRTs) are developed. The asymptotic distributions of the test statistics are also derived. In Section III the multicycle detectors are extended to allow collaborative detection by multiple secondary users. Censoring of the test statistics transmitted to the FC is considered in Section IV. Simulations results in multipath radio environments are given in Section V, and the paper is concluded in Section VI.

II. Single User Detection Using Multiple Cyclic Frequencies

Communication signals typically exhibit cyclostationarity at multiple cyclic frequencies. These cyclic frequencies may be related to symbol rate, coding and guard periods, or carrier frequency, for example. The cyclic frequencies present may vary depending on the waveforms used and on channel quality.

In order to benefit from the rich information present in typical communication signals, we extend the time domain second-order cyclostationarity test of [7] to multiple cyclic frequencies. In cognitive radio applications there typically exists prior information about the primary user waveforms. For example, the cyclic frequencies of the primary user signals (or at least some of them) are typically known since the waveforms are carefully specified in a standard. Hence, we assume the cyclic frequencies of the primary user signal to be known and focus on detecting the presence of the primary user signal rather than determining its cyclic frequencies.

A. Hypothesis Testing

In the following a test for a number of time delays as well as a set of cyclic frequencies of interest (e.g., for an orthog-

onal frequency division multiplex (OFDM) signal the cyclic frequencies of interest could be the symbol frequency and a few of its multiples) is constructed. The proposed tests are based on testing whether the expected value of the estimated cyclic autocorrelation is zero or not for the cyclic frequencies of interest. Let $\mathcal{A} = \{\alpha_n | n = 1, \ldots, P\}$ denote the set of cyclic frequencies of interest and

$$\begin{aligned}\hat{\boldsymbol{r}}_{xx^{(*)}} &= \Big[\mathrm{Re}\{\hat{R}_{xx^{(*)}}(\alpha_1, \tau_{1,1})\}, \ldots, \mathrm{Re}\{\hat{R}_{xx^{(*)}}(\alpha_1, \tau_{1,N_1})\}, \\ &\quad \mathrm{Im}\{\hat{R}_{xx^{(*)}}(\alpha_1, \tau_{1,1})\}, \ldots, \mathrm{Im}\{\hat{R}_{xx^{(*)}}(\alpha_1, \tau_{1,N_1})\}, \\ &\quad \cdots \\ &\quad \mathrm{Re}\{\hat{R}_{xx^{(*)}}(\alpha_P, \tau_{P,1})\}, \ldots, \mathrm{Re}\{\hat{R}_{xx^{(*)}}(\alpha_P, \tau_{P,N_P})\}, \\ &\quad \mathrm{Im}\{\hat{R}_{xx^{(*)}}(\alpha_P, \tau_{P,1})\}, \ldots, \mathrm{Im}\{\hat{R}_{xx^{(*)}}(\alpha_P, \tau_{P,N_P})\}\Big]\end{aligned} \tag{1}$$

denote a $1 \times 2N$ vector containing the real and imaginary parts of the estimated cyclic autocorrelations at the cyclic frequencies of interest stacked in a single vector. P is the number of cyclic frequencies in set $\mathcal{A}$ and $N = \sum_{n=1}^{P} N_n$ where $N_n, n = 1, \ldots, P$, are the number of time delays for each different cyclic frequency in (1). That is, cyclic autocorrelations for each cyclic frequency may be calculated for different time delays as well. The time delays are integer valued and $|\tau_{i,n}| < M, \forall i, n$, where M is the number of observations. The cyclic frequencies α_n can take on real value in the interval $[0, 1)$. Compared to [7](1) is an extension of $\hat{\boldsymbol{r}}_{xx^{(*)}}$ to multiple cyclic frequencies, each with a set of possibly distinct time delays. In [7], the cyclic autocorrelation vector $\hat{\boldsymbol{r}}_{xx^{(*)}}$ is given by

$$\begin{aligned}\hat{\boldsymbol{r}}_{xx^{(*)}} = \Big[&\mathrm{Re}\{\hat{R}_{xx^{(*)}}(\alpha, \tau_1)\}, \ldots, \mathrm{Re}\{\hat{R}_{xx^{(*)}}(\alpha, \tau_N)\}, \\ &\mathrm{Im}\{\hat{R}_{xx^{(*)}}(\alpha, \tau_1)\}, \ldots, \mathrm{Im}\{\hat{R}_{xx^{(*)}}(\alpha, \tau_N)\}\Big].\end{aligned} \tag{2}$$

An estimate of the (conjugate) cyclic autocorrelation $\hat{R}_{xx^{(*)}}(\alpha, \tau)$ may be obtained using M observations as

$$\hat{R}_{xx^{(*)}}(\alpha, \tau) = \frac{1}{M} \sum_{t=1}^{M} x(t) x^{(*)}(t + \tau) e^{-j2\pi\alpha t} \tag{3}$$

where $x(t)$ denotes the received complex valued signal, t is the discrete time index, and $(*)$ denotes an optional complex conjugation. The notation covers both cyclic autocorrelation and conjugate cyclic autocorrelation with only one expression. It is assumed that $x(t)$ has zero mean (in practice the mean can be estimated and subtracted from the signal). In addition, we assume the signal to be sufficiently oversampled. Oversampling at rate $f_s \geq 2KB$, where K is the order of cyclostationarity and B is the monolateral signal bandwidth (i.e., $[-B, B]$), guarantees that there is no aliasing in the cyclic frequency domain.

In order to test for the presence of second-order cyclostationarity at any of the cyclic frequencies of interest $\alpha \in \mathcal{A}$ simultaneously, the hypotheses are formulated as follows:

$$\begin{aligned}H_0 &: \hat{\boldsymbol{r}}_{xx^{(*)}} = \boldsymbol{\epsilon}_{xx^{(*)}}, \\ H_1 &: \hat{\boldsymbol{r}}_{xx^{(*)}} = \boldsymbol{r}_{xx^{(*)}} + \boldsymbol{\epsilon}_{xx^{(*)}}\end{aligned} \tag{4}$$

where $\boldsymbol{r}_{xx^{(*)}}$ is the nonrandom true cyclic autocorrelation vector. Furthermore, under commonly assumed circumstances (i.e., when samples well separated in time are approximately independent) $\boldsymbol{\epsilon}_{xx^{(*)}}$ is asymptotically normally distributed, i.e., $\lim_{M \to \infty} \sqrt{M} \boldsymbol{\epsilon}_{xx^{(*)}} \overset{D}{=} N(\boldsymbol{0}, \boldsymbol{\Sigma}_{xx^{(*)}})$ where $\boldsymbol{\Sigma}_{xx^{(*)}}$ is the $2N \times 2N$ asymptotic covariance matrix of $\hat{\boldsymbol{r}}_{xx^{(*)}}$. This result follows from [7] where the asymptotic normality of the cyclic autocorrelation estimator is established and the covariance of two cyclic autocorrelation estimates for arbitrary cyclic frequencies and time delays is derived. Hence, the extension to the above case is straightforward as well.

The asymptotic covariance matrix $\boldsymbol{\Sigma}_{xx^{(*)}}$ can be divided into $2N_\alpha \times 2N_\beta$ blocks, one block for each different cyclic frequency pair (α, β). Note that (α, β) is different from (β, α), although in practice symmetry can be used to reduce calculation. The $2N_\alpha \times 2N_\beta$ blocks $\bar{\boldsymbol{\Sigma}}_{xx^{(*)}}(\alpha, \beta)$ can be calculated as [7]

$$\boldsymbol{\Sigma}_{xx^{(*)}}(\alpha, \beta) = \begin{bmatrix} \mathrm{Re}\left\{\frac{\boldsymbol{Q}+\boldsymbol{P}}{2}\right\} & \mathrm{Im}\left\{\frac{\boldsymbol{Q}-\boldsymbol{P}}{2}\right\} \\ \mathrm{Im}\left\{\frac{\boldsymbol{Q}+\boldsymbol{P}}{2}\right\} & \mathrm{Re}\left\{\frac{\boldsymbol{P}-\boldsymbol{Q}}{2}\right\} \end{bmatrix}, \ \alpha, \beta \in \mathcal{A} \tag{5}$$

where the (m, n)th entries of the two covariance matrices $\boldsymbol{Q}$ and $\boldsymbol{P}$ are given by

$$\begin{aligned}\boldsymbol{Q}_{\alpha,\beta}(m, n) &= S_{f_{\tau_m} f_{\tau_n}}(\alpha + \beta, \beta) \\ \boldsymbol{P}_{\alpha,\beta}(m, n) &= S^*_{f_{\tau_m} f_{\tau_n}}(\alpha - \beta, -\beta).\end{aligned} \tag{6}$$

Here, $S_{f_{\tau_m} f_{\tau_n}}(\alpha, \omega)$ and $S^*_{f_{\tau_m} f_{\tau_n}}(\alpha, \omega)$ denote the nonconjugated and conjugated cyclic spectra of $f(t, \tau) = x(t) x^{(*)}(t + \tau)$, respectively. These spectra may be estimated, e.g., by using frequency smoothed cyclic periodograms as follows:

$$\begin{aligned}\hat{S}_{f_{\tau_m} f_{\tau_n}}(\alpha + \beta, \beta) = \frac{1}{MT} &\sum_{s=-(T-1)/2}^{(T-1)/2} W(s) \\ &\cdot F_{\tau_n}\left(\alpha - \frac{2\pi s}{M}\right) F_{\tau_m}\left(\beta + \frac{2\pi s}{M}\right)\end{aligned} \tag{7}$$

and

$$\begin{aligned}\hat{S}^*_{f_{\tau_m} f_{\tau_n}}(\alpha - \beta, -\beta) = \frac{1}{MT} &\sum_{s=-(T-1)/2}^{(T-1)/2} W(s) \\ &\cdot F^*_{\tau_n}\left(\alpha + \frac{2\pi s}{M}\right) F_{\tau_m}\left(\beta + \frac{2\pi s}{M}\right)\end{aligned} \tag{8}$$

where $F_\tau(\omega) = \sum_{t=1}^{M} x(t) x^{(*)}(t + \tau) e^{-j\omega t}$ and W is a normalized spectral window of odd length T.

In the following the GLRT and its asymptotic distribution are derived. We begin from the likelihood ratio and derive the GLRT statistic. Finally, we employ an asymptotic theorem to obtain the distributions under both hypotheses. The distributions derived here are extensions to multiple cyclic frequencies of the ones derived in [7]. The asymptotics for the single cyclic frequency situation derived in [7] are obtained as a special case. In addition, the distribution under H_1 derived here is more accurate than the one in [7]. As we will later explain, the distribution under H_1 provided in [7] is obtained from the distribution derived here using a normal approximation.

B. Generalized Likelihood Ratio Test (GLRT)

Using the asymptotic normality of $\hat{\boldsymbol{r}}_{xx^{(*)}}$, the likelihood ratio (LR) is given by (note that there is only one observation of $\hat{\boldsymbol{r}}_{xx^{(*)}}$)

$$\Lambda = \frac{f(\hat{\boldsymbol{r}}_{xx^{(*)}}|H_1)}{f(\hat{\boldsymbol{r}}_{xx^{(*)}}|H_0)} = \frac{\exp(-\frac{1}{2}M(\hat{\boldsymbol{r}}_{xx^{(*)}}-\boldsymbol{r}_{xx^{(*)}})\boldsymbol{\Sigma}_{xx^{(*)}}^{-1}(\hat{\boldsymbol{r}}_{xx^{(*)}}-\boldsymbol{r}_{xx^{(*)}})^T)}{\exp(-\frac{1}{2}M\hat{\boldsymbol{r}}_{xx^{(*)}}\boldsymbol{\Sigma}_{xx^{(*)}}^{-1}\hat{\boldsymbol{r}}_{xx^{(*)}}^T)}. \tag{9}$$

The generalized likelihood ratio (GLR) is obtained by substituting $\hat{\boldsymbol{r}}_{xx^{(*)}}$ for $\boldsymbol{r}_{xx^{(*)}}$ and $\hat{\boldsymbol{\Sigma}}_{xx^{(*)}}$ for $\boldsymbol{\Sigma}_{xx^{(*)}}$, i.e.,

$$\tilde{\Lambda} = \exp\left(\frac{1}{2}M\hat{\boldsymbol{r}}_{xx^{(*)}}\hat{\boldsymbol{\Sigma}}_{xx^{(*)}}^{-1}\hat{\boldsymbol{r}}_{xx^{(*)}}^T\right). \tag{10}$$

The final generalized log-likelihood ratio test statistic is obtained by taking the logarithm and multiplying the result by 2, i.e.,

$$\mathcal{T}_{xx^{(*)}} = 2\ln\tilde{\Lambda} = M\hat{\boldsymbol{r}}_{xx^{(*)}}\hat{\boldsymbol{\Sigma}}_{xx^{(*)}}^{-1}\hat{\boldsymbol{r}}_{xx^{(*)}}^T. \tag{11}$$

In case set $\mathcal{A}$ contains only one cyclic frequency then the test statistic in (11) reduces to the test statistic in [7].

C. Asymptotic Distribution of the GLR Test Statistic

In order to derive the asymptotic distribution of the GLR test statistic, the following theorem is employed [23].

Theorem 1: Let $\boldsymbol{x} \sim N(\boldsymbol{\mu}, \boldsymbol{V})$, where $\boldsymbol{V}$ is $p \times p$ nonsingular, suppose that the real $p \times p$ matrix $\boldsymbol{A}$ is symmetric, and let $r(\boldsymbol{A})$ denote its rank. Then the quadratic form $\boldsymbol{x}\boldsymbol{A}\boldsymbol{x}^T$ follows a chi-square distribution if and only if $\boldsymbol{A}\boldsymbol{V}$ is idempotent, in which case $\boldsymbol{x}\boldsymbol{A}\boldsymbol{x}^T$ has $r(\boldsymbol{A})$ degrees of freedom and noncentrality parameter $\boldsymbol{\mu}\boldsymbol{A}\boldsymbol{\mu}^T$.

Here $\boldsymbol{x} = \sqrt{M}\hat{\boldsymbol{r}}_{xx^{(*)}}$, $\boldsymbol{\mu} = \boldsymbol{0}$ under H_0 and $\boldsymbol{\mu} = \sqrt{M}\boldsymbol{r}_{xx^{(*)}}$ under H_1, $\boldsymbol{V} = \boldsymbol{\Sigma}_{xx^{(*)}}$, and $\boldsymbol{A} = \hat{\boldsymbol{\Sigma}}_{xx^{(*)}}^{-1}$. Since $\hat{\boldsymbol{\Sigma}}_{xx^{(*)}}^{-1}$ is mean-square sense convergent [7], i.e., $\lim_{M\longrightarrow\infty}\hat{\boldsymbol{\Sigma}}_{xx^{(*)}}^{-1} \overset{m.s.s}{=} \boldsymbol{\Sigma}_{xx^{(*)}}^{-1}$, $\lim_{M\longrightarrow\infty}\boldsymbol{A}\boldsymbol{V} = \lim_{M\longrightarrow\infty}\hat{\boldsymbol{\Sigma}}_{xx^{(*)}}^{-1}\boldsymbol{\Sigma}_{xx^{(*)}} \overset{P}{=} \boldsymbol{\Sigma}_{xx^{(*)}}^{-1}\boldsymbol{\Sigma}_{xx^{(*)}} = \boldsymbol{I}$ and thus the matrix product is asymptotically idempotent. The convergence in probability follows from application of a Cramér–Wold device (e.g., [24, p. 147]) and from the fact that convergence in the mean-square implies convergence in probability. Hence, from Theorem 1 it follows that under H_0

$$\lim_{M\longrightarrow\infty}\mathcal{T}_{xx^{(*)}} \overset{D}{=} \chi_{2N}^2 \tag{12}$$

and under H_1 we can approximately write for large M

$$\mathcal{T}_{xx^{(*)}} \sim \chi_{2N}^2(M\boldsymbol{r}_{xx^{(*)}}\hat{\boldsymbol{\Sigma}}_{xx^{(*)}}^{-1}\boldsymbol{r}_{xx^{(*)}}^T) \tag{13}$$

where $N = \sum_{n=1}^{P} N_n$.

That is, under the null hypothesis $\mathcal{T}_{xx^{(*)}}$ is asymptotically (central) chi-square distributed with $2N$ degrees of freedom and under the alternative hypothesis noncentral chi-square distributed with $2N$ degrees of freedom and noncentrality parameter $M\boldsymbol{r}_{xx^{(*)}}\hat{\boldsymbol{\Sigma}}_{xx^{(*)}}^{-1}\boldsymbol{r}_{xx^{(*)}}^T$.

The normal distribution approximation under H_1 for the single cyclic frequency case derived in [7] follows from (13) with a normal approximation and assuming that $M\boldsymbol{r}_{xx^{(*)}}\hat{\boldsymbol{\Sigma}}_{xx^{(*)}}^{-1}\boldsymbol{r}_{xx^{(*)}}^T \gg N$. Note that this may not be a very reasonable assumption in the low SNR regime when the value of $M\boldsymbol{r}_{xx^{(*)}}\hat{\boldsymbol{\Sigma}}_{xx^{(*)}}^{-1}\boldsymbol{r}_{xx^{(*)}}^T$ can be relatively small compared to N.

The test is now defined as follows. Accept H_1 if $\mathcal{T}_{xx^{(*)}} > \gamma$, where γ is the test threshold chosen so that $p_{fa} = p(\mathcal{T}_{xx^{(*)}} > \gamma|H_0)$, and p_{fa} is the false alarm rate parameter.

D. Computationally Efficient Test Statistics

The Fourier coefficients of a wide-sense stationary random process for different frequencies are asymptotically uncorrelated [22]. Moreover, the Fourier coefficients of a Gaussian random process are asymptotically independent. Since the cyclic autocorrelation estimates are the Fourier coefficients of the autocorrelation function, they are asymptotically uncorrelated for different cyclic frequencies. Under the null hypothesis there is no cyclostationarity present. Thus, the cyclic correlation estimates at different cyclic frequencies (i.e., the Fourier coefficients) are asymptotically uncorrelated. Hence, under the null hypothesis $\boldsymbol{\Sigma}_{xx^{(*)}}$ is a block-diagonal matrix. Consequently, the test statistic in (11) simplifies to

$$\mathcal{D}_s = \mathcal{T}_{xx^{(*)}} = \sum_{\alpha\in\mathcal{A}}\mathcal{T}_{xx^{(*)}}(\alpha) \tag{14}$$

where $\mathcal{T}_{xx^{(*)}}(\alpha)$ denotes the cyclostationary test statistic calculated for single cyclic frequency α in the set of cyclic frequencies of interest $\mathcal{A}$. Note that the asymptotic distribution under the null hypothesis remains the same.

Using (14) instead of (11) is computationally more efficient especially if the number of cyclic frequencies of interest in the set $\mathcal{A}$ is large (more than 3 or 4). However, since the whole correlation structure of the signal is not taken into account the detection performance may degrade. On the other hand, depending on the signal and employed cyclic frequencies, in the high SNR regime, the cyclic autocorrelation estimates for different cyclic frequencies may be linearly dependent. If the full correlation structure is taken into account this may cause problems in the detection since it may make the estimated covariance matrix rank deficient. This problem may be avoided by removing one of the linearly dependent parameters. In practice, as will be demonstrated in the simulation section, there is not a significant difference in detection performances between the full and simplified models.

The multicycle detector of (11) and the multicycle sum detector of (14) are best suited for situations where the primary signal has multiple strong cyclic frequencies. That is, the primary signal exhibits significant spectral correlation at these cyclic frequencies. Otherwise the performance may deteriorate since each test statistic for different cyclic frequency increases the number of degrees of freedom of the asymptotic distribution. Consequently, including cyclic frequencies that do not provide substantial contribution is not beneficial.

Another interesting test statistic is obtained by calculating the maximum of the cyclostationary test statistic over the set of cyclic frequencies of interest, i.e.,

$$\mathcal{D}_m = \max_{\alpha\in\mathcal{A}}\mathcal{T}_{xx^{(*)}}(\alpha). \tag{15}$$

Finding the maximum over the cyclic frequencies of interest may prove to be useful if the cyclic frequencies are due to different signal properties or if the primary user system has multiple alternating operation modes that result in different cyclic frequencies. For example, adaptive modulation and coding may lead to such signals.

Under the null hypothesis the asymptotic cumulative distribution function (cdf) of $\mathcal{D}_m$ is given by

$$F_{\mathcal{D}}(x,P,\{N_i\}_{i=1}^{P})=\prod_{i=1}^{P}\left(1-e^{-x/2}\sum_{n=0}^{N_i-1}\frac{\left(\frac{x}{2}\right)^n}{n!}\right). \quad (16)$$

The null hypothesis is rejected if $F_{\mathcal{D}}(x,P,\{N_i\}_{i=1}^{P})>1-p_{fa}$ where p_{fa} is the false alarm rate and P is the number of tested cyclic frequencies. See the Appendix for detailed derivation.

III. Collaborative Detection

In cognitive radio systems, there are typically multiple spatially distributed secondary users that are trying to find underutilized spectrum, i.e., spectral holes. User cooperation can be realized in a number of different ways. All the secondary users may sense the entire band of interest, or in order to reduce power consumption monitor just a partial band. In the latter case each secondary user senses a certain part of the spectrum, and then shares the acquired information with other users or an FC. With multiple spatially distributed users sensing each frequency band, the diversity gains necessary for mitigating the shadowing and fading effects can be achieved. Here, the focus is on collaboration of a group of secondary users all sensing the same frequency band.

In addition to being coordinated by an FC, the cooperation may take place in an ad hoc manner without a dedicated FC, i.e., the secondary users distribute their local quantized information to all the other users and each user performs the fusion locally. Here it is assumed that an FC collects information from all L secondary users and makes a decision about whether the frequency band is available or not. Each secondary user sends a quantized version of its local spectrum sensing statistics (such as the LR) to the FC. In the case of very coarse quantization, binary local decision may be sent. Assuming that the secondary users are independent given H_0 or H_1, the optimal fusion rule is the LR test over the received local LRs Λ_i:

$$\Lambda_L=\prod_{i=1}^{L}\Lambda_i. \quad (17)$$

In case the secondary users send binary decisions, the sum of ones may be calculated and compared to a threshold. Here, a simple way of making the decision using GLRs is considered. Note that due to using GLRs optimality cannot be claimed.

Equivalently to the product of the LRs, (17) can be written as the sum of log-LRs. Hence, the following test statistic is obtained:

$$\mathcal{T}_L=\sum_{i=1}^{L}\mathcal{T}_{xx^{(*)}}^{(i)} \quad (18)$$

where $\mathcal{T}_{xx^{(*)}}^{(i)}$ is either the full correlation test statistic in (11) or the simplified sum test statistic in (14) of user i.

In addition, the following maximization test statistic is proposed:

$$\mathcal{D}_{m,L}=\max_{\alpha\in\mathcal{A}}\sum_{i=1}^{L}\mathcal{T}_{xx^{(*)}}^{(i)}(\alpha). \quad (19)$$

Under the conditional independence assumption the asymptotic distribution of the test statistic $\mathcal{T}_L$ in (18) is χ^2_{2NL} under the null hypothesis. This is due to the fact that the sum of independent chi-square random variables is also a chi-square random variable whose degrees of freedom is the sum of the degrees of freedom of the independent random variables. The cumulative distribution function of $\mathcal{D}_{m,L}$ in (19) is $F_{\mathcal{D}}(\mathcal{D}_{m,L},P,\{N_iL\}_{i=1}^{P})$ under the null hypothesis where P is the number of tested cyclic frequencies.

A censoring scheme for reducing the amount of transmitted data, taking into account the relevance of the information provided by secondary users as well as how to deal with communication rate constraints, will be introduced in the following section.

IV. Collaborative Detection With Censoring

In a collaborative spectrum sensing scheme the transmission of the spectrum sensing results by the secondary users to an FC or other secondary users in ad hoc scenarios generates substantial overhead traffic. A significant reduction in the amount of data transmitted may be achieved by transmitting only the relevant or informative test statistics to the FC or the other users. This operation is called censoring. It reduces the energy consumption of the secondary user terminals since fewer terminals are transmitting at any given time. In the following a censoring strategy for cyclostationarity based spectrum sensing under communication rate constraints is proposed. Censoring has been employed in energy efficient sensor networks in [18] and [19].

Let L denote the total number of collaborating secondary users and K denote the number of users transmitting their test statistics to the FC or the user making the decision. Each user is assigned a separate communication rate constraint defined by

$$p\left(\mathcal{T}_{xx^{(*)}}^{(i)}>t_i\middle|H_0\right)\le\kappa_i,\ i=1,\ldots,L \quad (20)$$

where $\kappa_i\in[0,1]$ is the communication rate constraint of user i and t_i is the upper limit of the censoring (no-send) region of the user i. That is, each user will transmit its test statistic to the FC only if its value is above t_i where t_i is chosen such that the probability of the user i transmitting the test statistic to the FC under H_0 is κ_i. This type of strategy in which each user is assigned a separate communication rate constraint has been suggested in [19] for censoring in sensor networks. The choice is natural in a scenario where the secondary user terminals may have very different capabilities for data transmission. Moreover, the threshold values t_i needed to meet the communication rate constraints can easily be selected independently by the secondary users. Recall that under the null hypothesis H_0 the test statistic

$\mathcal{T}^{(i)}_{xx^{(*)}}$ in (20) is asymptotically χ^2_{2N} distributed. However, the threshold values (or the communication rate constraints) must be communicated to the FC. Note that the maximum achievable false alarm rate without randomization for this strategy is given by $1-\prod_{i=1}^{L}(1-\kappa_i)$.

The test statistic of the proposed censoring test is given by

$$\mathcal{D}_L = \sum_{i=1}^{K} \mathcal{T}^{(i)}_{xx^{(*)}} + \sum_{i=1}^{L-K} d_i = \mathcal{D}_K + \sum_{i=1}^{L-K} d_i \qquad (21)$$

where the latter sum corresponds to the generalized log-LRs in the no-send region. The idea is that the test statistics of the secondary users not transmitting are replaced by a constant value denoted by d_i. Here, the value chosen for d_i is the conditional mean of the local generalized log-LR of the ith user (i.e., the test statistic $\mathcal{T}^{(i)}_{xx^{(*)}}$) in the no-send region under H_0, i.e.,

$$d_i = E\left[\mathcal{T}^{(i)}_{xx^{(*)}} \middle| \mathcal{T}^{(i)}_{xx^{(*)}} \le t_i, H_0\right], \quad i=1,\ldots,L. \qquad (22)$$

Since $\mathcal{T}^{(i)}_{xx^{(*)}}$ is under the null hypothesis χ^2_{2N} distributed random variable, the value of d_i is easily obtained at the FC using the threshold t_i [that is defined by the communication rate constraint κ_i, see (20)]. Thus, there is no need to transmit d_i. The communication rate constraint κ_i is the only parameter transmitted to the FC.

Determining the value of d_i can be considered as quantization to only one value. In other words, the whole distribution of values in the no-send region is represented by a single value. With this analogy it is obvious that choosing the conditional mean as the value for d_i is optimal in the minimum mean-square error (MMSE) sense. Finally, note that although the value of d_i is constant and can be set offline, the value of the second sum in (21) is a random variable since K is random. Hence, the second sum cannot be included in the test threshold if a single threshold is used for all K.

Here only FC test statistics based on summation of local test statistics of the secondary users are employed. Maximization over the cyclic frequencies of interest at the FC requires transmission of test statistics for all cyclic frequencies. Thus, it generates P times more data than summation based test statistics where P is the number of cyclic frequencies of interest.

To summarize, apart from the secondary user test statistics exceeding the censoring thresholds, the only additional information that has to be transmitted to the FC during the censoring process is the set of communication rate constraints κ_i (or alternatively the censoring thresholds t_i). Moreover, each communication rate constraint κ_i has to be transmitted only once when the cooperation is initiated and afterwards only whenever it is changed.

Censoring affects the distribution of the global test statistic at the FC or secondary user where the statistics are combined. Essentially, the task is to determine the distribution of a sum of truncated chi-square distributed random variables.

The distribution of the test statistic $\mathcal{D}_L$ can be defined using conditional distributions as follows:

$$p(\mathcal{D}_L|H_0) = \sum_{k=0}^{L} p(\mathcal{D}_L|K=k,H_0)p(K=k|H_0) \qquad (23)$$

where the probabilities of different values of K are obtained by enumerating all possible combinations and computing their respective probabilities. In case all the secondary users have equal communication rate constraints, i.e., $\kappa=\kappa_i,\ \forall i$, then the probabilities are given by

$$p(K=k|H_0) = \binom{L}{k}\kappa^k(1-\kappa)^{L-k}. \qquad (24)$$

Now let us consider only the terms $\mathcal{T}^{(i)}_{xx^{(*)}}$ of the first sum in (21). The probability density function (pdf) of $y=\mathcal{T}^{(i)}_{xx^{(*)}}$ at the FC is given by a truncated chi-square pdf, i.e.,

$$g(y,2N|H_0) = \frac{1}{1-G(t)}\cdot\frac{1}{2^N\Gamma(N)}y^{N-1}e^{-y/2}, y\ge t \qquad (25)$$

where $2N$ is the number of degrees of freedom and $\Gamma(\cdot)$ denotes the gamma function. The censoring threshold (i.e., the upper limit of the censoring region) is denoted by t and $G(\cdot)$ denotes the cumulative distribution function of the chi-square distribution. For $y<t$, $g(y,2N|H_0)=0$.

Determining the distribution of a sum of truncated chi-square distributed random variables in a closed form is very difficult. Here, the fact that the cumulative distribution function may be obtained by inverting the characteristic function is employed to approximate the distribution numerically. One form of the inversion theorem between the characteristic function $\Phi(\cdot)$ and the cumulative distribution function $F(\cdot)$ is given by [25]

$$F(y) = \frac{1}{2} - \int_{-\infty}^{\infty}\frac{\Phi(\omega)}{j2\pi\omega}e^{-j\omega y}d\omega \qquad (26)$$

where j denotes the imaginary unit. Before the actual method employed for the numerical inversion of the characteristic function is presented, the characteristic function of the test statistic is derived.

The characteristic function of a random variable Y is defined by

$$\Phi(\omega) = E[\exp(j\omega y)] \qquad (27)$$

where $E[\cdot]$ denotes the expectation operator. The characteristic function always exists. Moreover, it uniquely defines the distribution of the random variable.

Using (27) the characteristic function of the truncated chi-square pdf is defined by

$$\Phi_{\mathcal{T}}(\omega) = \int_t^{\infty}\exp(j\omega y)g(y,2N|H_0)dy. \qquad (28)$$

Using repeated integration by parts the following result is obtained

$$\Phi_{\mathcal{T}}(\omega) = \frac{1}{1-G(t)}\sum_{n=1}^{N}\left(\frac{1}{(N-n)!}2^{-N+n}t^{N-n}\cdot(1-2j\omega)^{-n}\exp\left(\frac{-(1-2j\omega)t}{2}\right)\right). \qquad (29)$$

Since the individual test statistics $\mathcal{T}^{(i)}_{xx^{(*)}}$ are independent, the characteristic function of the first sum in (21) (i.e., the characteristic function of $\mathcal{D}_K$) factors to a product of the characteristic

functions of the individual test statistics. That is, the characteristic function of $\mathcal{D}_K$ for a given $K = k$ is given by

$$\Phi_{\mathcal{D}_k}(\omega) = \prod_{i=1}^{k} \Phi_{\mathcal{T}_i}(\omega). \tag{30}$$

For equal communication rate constraints among the secondary users, the characteristic function of $\mathcal{D}_K$ for a given $K = k$ is given by

$$\Phi_{\mathcal{D}_k}(\omega) = \Phi_{\mathcal{T}}(\omega)^k. \tag{31}$$

Finally, the characteristic function of $\mathcal{D}_L$ for a given $K = k$ is given by $\Phi_{\mathcal{D}_L}(\omega) = \exp(j\omega \sum_{i=1}^{L-k} d_i)\Phi_{\mathcal{D}_k}(\omega)$. The result follows directly from (27) since the d_i's are nonrandom.

The distributions $p(\mathcal{D}_L|K = k, H_0)$ can be approximated by numerically inverting the characteristic function. Here a Fourier-series method introduced in [26] for numerical inversion of the characteristic function is employed. The chosen method is very simple and easy to use. Although there exists many more sophisticated and accurate methods, the accuracy of the chosen method is more than sufficient for the application at hand. For a comprehensive review of Fourier-series methods for numerical inversion of characteristic functions, Laplace transforms, and generating functions, see [27].

The value of cumulative distribution function $F(y)$ of a random variable Y with zero mean and unit variance can be approximated by [26]

$$F(y) \approx \frac{1}{2} + \frac{\eta y}{2\pi} - \sum_{\substack{\nu=1-H \\ \nu \neq 0}}^{H-1} \frac{\Phi_Y(\eta\nu)}{2\pi j\nu} e^{-j\eta\nu y} \tag{32}$$

where $\Phi_Y(\cdot)$ denotes the characteristic function of Y. The distribution is approximated at $2H-1$ different points. η is a constant chosen such that the full range of the distribution is represented (i.e., values of $F(y)$ include both 0 and 1). In order to be able to use the fast-Fourier transform (FFT) to calculate the sum in (32) the points y are chosen as the Fourier frequencies, i.e., $y_k = 2\pi(k-H)/(2\eta(H-1))$, $k = 1, \ldots, 2H-1$. Note that the undefined value for index $\nu = 0$ has to be excluded from the final sum.

Since (32) is defined for a normalized random variable with a mean zero and unit variance, the test statistic has to be normalized as well. The mean and variance can be easily calculated by differentiating the characteristic function since $\Phi_Y^{(n)}(0) = j^n E[y^n]$ and the variance $\sigma^2 = E[y^2] - E[y]^2$. The mean and variance of a truncated chi-square distributed random variable Y with pdf defined by (25) are given by

$$\mu = \frac{1}{1-G(t)} \sum_{n=1}^{N} \frac{(2n+t)}{(N-n)!} 2^{-N+n} t^{N-n} e^{-t/2} \tag{33}$$

and

$$\sigma^2 = \frac{1}{1-G(t)} \sum_{n=1}^{N} \left(\frac{1}{(N-n)!} 2^{-N+n} t^{N-n} e^{-t/2} \cdot (4n(n+1) + 4nt + t^2) \right) - \mu^2. \tag{34}$$

Since the test statistics of the secondary users are independent, the mean and variance of the FC test statistic are obtained by summing the mean and variances of the secondary user test statistics, respectively. Note that for the mean of the FC test statistic the term $\sum_{i=1}^{L-k} d_i$ in (21) has to be added as well. The variance does not change since the d_i are nonrandom. Finally, the characteristic function of a normalized variable $Z = (Y-\mu)/\sigma$ is given by $\Phi_Z(\omega) = \exp(-j\omega\mu/\sigma)\Phi_Y(\omega/\sigma)$.

The distributions $p(\mathcal{D}_L|K = k, H_0)$ can be approximated by using (32). The combined distribution $p(\mathcal{D}_L|H_0)$ is obtained by multiplying the conditional distributions with the probabilities of different values of K. The distribution values between the FFT points can be interpolated.

In order to obtain a desired false alarm rate p_{fa}, a single test threshold γ may be set using the following equation:

$$p_{fa} = p(\mathcal{D}_L > \gamma | H_0). \tag{35}$$

Alternatively, different thresholds may be used for different values of the number of received test statistics K. The desired false alarm rate is obtained if the thresholds γ_k, $k = 1, \ldots, L$, satisfy the following condition:

$$p_{fa} = \sum_{k=1}^{L} p(\mathcal{D}_L > \gamma_k | K = k, H_0) p(K = k | H_0). \tag{36}$$

In the above expression, it is assumed that if none of the users transmits, the decision is always H_0. For example, the thresholds γ_k may be chosen such that $p(\mathcal{D}_L > \gamma_k|K = k, H_0) = p_{fa}/\sum_{k=1}^{L} p(K = k|H_0), \forall k$. Furthermore, a constant false alarm rate (CFAR) can be maintained also if the thresholds are defined by $p(\mathcal{D}_L > \gamma_k|K = k, H_0) = p_{fa}$. This is a nonoptimal strategy but may be used if the total number of collaborating users is not known (note that the communication rate constraints still need to be known). In that case the combined distribution $p(\mathcal{D}_L|H_0)$ does not have to be calculated since only the conditional distributions $p(\mathcal{D}_L|K = k, H_0)$ are required. Note that in this case it is necessary to use $d_i = 0, \forall i$, since the number of users not transmitting is not known.

In case the communication rate constraints are chosen equal for each secondary user, i.e., $\kappa = \kappa_i, \forall i$, the amount of required computation is considerably reduced. If the communication rate constraints are not equal, the approximation of the distributions $p(\mathcal{D}_L|K = k, H_0)$ means that the Fourier-series approximation has to be done for all different combinations of different users transmitting (and then combining the cdfs using their respective probabilities). Hence, from a practical point of view it is advisable to limit the number of different communication rate constraints the secondary users can select in order to reduce the number of different combinations.

Finally, we point out that the proposed censoring scheme may be directly applied also to other test statistics that are under the null hypothesis chi-square distributed, such as the energy detector.

V. Simulation Examples

The primary user signal considered in the simulations is the OFDM signal. OFDM is employed by many of the current as well as future wireless communications systems. OFDM

based systems include 3GPP Long term evolution (LTE), IEEE 802.11a/g Wireless local area networks (WLAN), Digital video broadcasting (DVB) standards DVB-T and DVB-H, as well as IEEE 802.16 and WiMax Wireless metropolitan area networks (MAN), for example. A baseband OFDM signal is given by

$$x(t) = \sum_{n=0}^{N_c-1} \sum_{l=-\infty}^{\infty} c_{n,l} g(t - lT_s) e^{j(2\pi/N_c)n(t-lT_s)} \quad (37)$$

where N_c is the number of subcarriers, T_s is the symbol length, $g(t)$ denotes the rectangular pulse of length T_s, and $c_{n,l}$'s denote the data symbols. The symbol length is given by $T_s = T_d + T_{\text{cp}}$ where T_d is the length of the useful symbol data and T_{cp} the length of the cyclic prefix.

In addition to possibly other cyclic frequencies, a cyclic prefix OFDM signal exhibits cyclostationarity at the integer multiples of the symbol rate $\alpha = k/T_s$, $k = 0, \pm 1, \pm 2, \ldots$. In the following simulation experiments the single cycle detector employs the cyclic frequency of $1/T_s$ while the multicycle detectors employ $1/T_s$ and $2/T_s$. Furthermore, if not otherwise mentioned all the detectors use two time lags $\pm T_d$. That is, the detectors assume the knowledge of the symbol frequency and the useful symbol length. The cyclic autocorrelation of the OFDM signal has a peak for the above time lags [8].

The cyclic spectrum estimates were calculated using a length 2049 Kaiser window with β parameter of 10. The Fourier-series method for approximating the cdfs of the FC test statistics after censoring employs the parameter values $\eta = 0.5$ and $H = 1000$ (see (32) and the explanation after it). The plotted simulation curves are averages over 1000 experiments.

Detection performance is measured as a function of the SNR. The SNR in decibels is defined by

$$\text{SNR(dB)} = 10 \log_{10} \frac{\sigma_x^2}{\sigma_n^2} \quad (38)$$

where σ_x^2 and σ_n^2 are the powers of the transmitted signal and the noise, respectively. The channels are normalized to have an expected channel gain of one. In all of the simulations the secondary users experience independent channels (i.e., fading and shadowing) and receiver noises. However, the statistics of the fading, shadowing, and noise processes are identical among secondary users.

A. *Theoretical Analysis versus Simulation Results*

Fig. 1 illustrates the accuracy of the asymptotic distribution under the null hypothesis in (12) for the multicycle detectors in (11) and (14). In the figure the theoretical cdf of the χ^2_{2N} distribution with $N = 4$ and simulated empirical cdfs for white Gaussian noise for two different number of samples have been plotted. Already with 1000 samples the accuracy of the asymptotic distribution is very good. The accuracy of the asymptotic distribution for the simplified sum test statistic is slightly worse with 1000 samples in the most important region for detection, the upper tail of the distribution, than for the test statistic that takes the correlations between the different cyclic frequencies into account. The sum test statistic requires slightly more samples for the asymptotic distribution to hold true in the upper tail of the distribution.

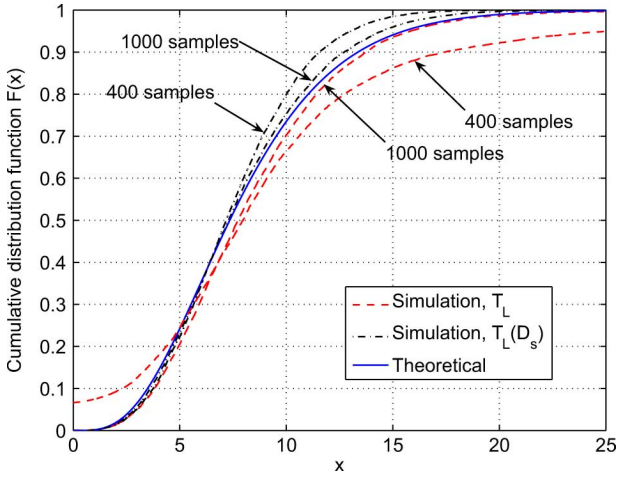

Fig. 1. Comparison of theoretical and simulated cdfs for white Gaussian noise (i.e., under H_0) for two different number of samples. As the number of samples increases the accuracy of the theoretic asymptotic distribution improves. The detectors use two random cyclic frequencies and two random time delays. The theoretical cdf has been obtained using the distribution in (12).

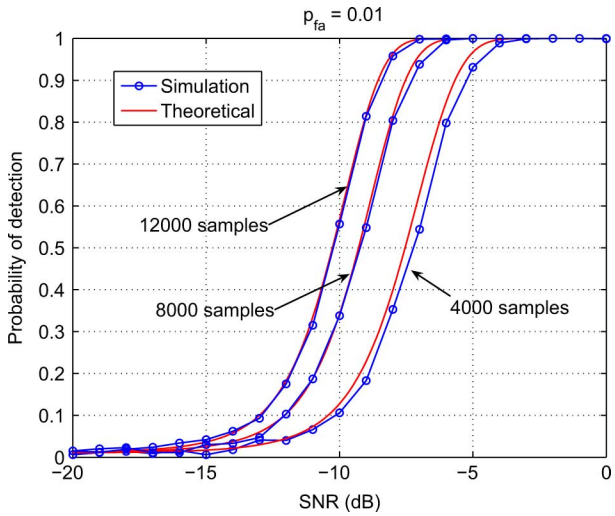

Fig. 2. Comparison of theoretical and simulated performance curves for a WLAN OFDM signal in AWGN for three different signal lengths. As the number of samples increases the accuracy of the theoretic asymptotic distribution improves. The theoretical and simulation curves practically overlap with 12 000 samples. The signal lengths in time are 0.2, 0.4, and 0.6 ms. The detectors use two cyclic frequencies and one time delay equal to N_{FFT}. The theoretical curves have been obtained using the distribution in (13).

Fig. 2 compares theoretical and simulated performance curves for a WLAN OFDM signal in additive white Gaussian noise (AWGN) for 3 different number of samples. The number of subcarriers $N_{\text{FFT}} = 64$ of which $N_{\text{occ}} = 52$ are occupied, and the cyclic prefix length $N_{\text{cp}} = 16$. The subcarrier modulation is QPSK (quadrature phase shift keying). The false alarm rate $p_{\text{fa}} = 0.01$. The signal was sampled at the Nyquist rate; that is, the oversampling factor with respect to the symbol rate is $N_{\text{FFT}} + N_{\text{cp}}$. The accuracy of the theoretical asymptotic distribution improves as the number of samples increases. The asymptotics start to hold very accurately when the number of samples approaches 12 000. The number of samples required for the asymptotic distribution to hold true depends also on the signal and its characteristics and the sampling rate. Note that

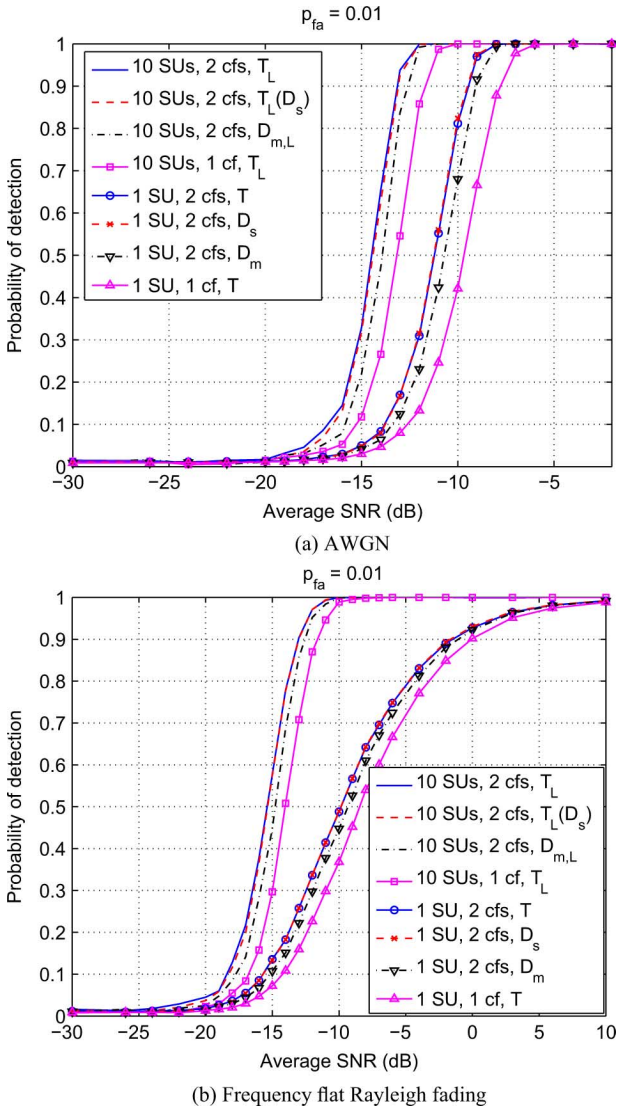

(a) AWGN

(b) Frequency flat Rayleigh fading

Fig. 3. Probability of detection versus SNR (dB) for a DVB-T signal in (a) AWGN and (b) frequency flat Rayleigh fading channels. Collaboration among secondary users improves performance through diversity. It mitigates the effects of fading. Using multiple frequencies further improves the detection performance. (SU = secondary user, cf = cyclic frequency).

the fact that the asymptotic distributions under H_1 do not necessarily hold true for small number of samples does not mean that the algorithm cannot be used if the sample size is not large enough. Merely, the performance cannot be predicted using the theoretical curves. The more important factor is the accuracy of the asymptotic distribution under H_0 which holds true for far less number of samples (roughly 1000). This guarantees the CFAR nature of the algorithm.

B. Multicycle and Collaborative Detection

Fig. 3 depicts the performance of the proposed multicycle detectors as a function of the SNR for a DVB-T (Digital video broadcasting, Terrestrial television) signal in (a) AWGN and (b) frequency flat Rayleigh fading channels. The DVB-T signal parameters are as follows: $N_{\mathrm{FFT}} = 8192$, $N_{\mathrm{occ}} = 6817$, and $N_{\mathrm{cp}} = 1024$. The subcarrier modulation is 64-QAM (quadrature amplitude modulation). The length of the signal is three OFDM symbols ($\approx$ 3 ms). The signal was sampled at the Nyquist rate; that is, the oversampling factor with respect to the symbol rate is $N_{\mathrm{FFT}} + N_{\mathrm{cp}}$. Thus, the number of samples is $3 \times (N_{\mathrm{FFT}} + N_{\mathrm{cp}}) = 27\,648$ samples. The same sampling strategy is used in all of the following simulations as well.

The figures show that in order to obtain reliable performance in challenging propagation environments, collaboration among secondary users is necessary. The performance for a single secondary user operating alone is significantly worse in Rayleigh fading channel than in AWGN. Collaboration among secondary users brings the overall detection performance in Rayleigh fading on the same level with the overall collaborative detection performance in AWGN. Collaboration provides spatial diversity and thus reduces the impact of fading on the overall detection performance. That is, the probability that every secondary user is simultaneously in a deep fade is smaller as the number of spatially displaced secondary users increases. Using multiple cyclic frequencies further improves the performance. The performance improvement is 1–2 dB. The gain obtained from collaboration is far greater. In addition, it can be seen that taking into account the full correlation structure between estimates at different cyclic frequencies provides the best performance. However, the performance difference to the best simplified multicycle detector, the sum detector $\mathcal{D}_s$, is not significant. Hence, in the following simulations the multicycle detectors are all sum detectors.

C. Comparison to Energy Detection

In the following we will compare the proposed cyclic detectors to energy detector in AWGN. The primary user signal is an IEEE 802.11a/g WLAN OFDM signal. The primary user signal parameters are as follows: $N_{\mathrm{FFT}} = 64$, $N_{\mathrm{occ}} = 52$, and $N_{\mathrm{cp}} = 16$. The subcarrier modulation is 64-QAM. The sensing time is 1 ms (= 20 000 samples).

We have implemented an energy detector that estimates the noise power from the guard bands. In order to obtain tolerance against carrier frequency offsets and leakage from the possibly occupied spectrum, we employ a noise power estimator that estimates the average power in 3 of the unoccupied subcarrier frequencies at both ends of the spectrum (i.e., six subcarrier frequencies in total). The obtained noise power estimate is employed in the energy detector to make it a CFAR detector. In addition, we consider the energy detector with known noise power and noise uncertainty denoted by Δ in decibels (i.e., noise power $\pm\Delta$).

Fig. 4 depicts the performance of the detectors for the primary user signal as a function of the SNR. The energy detector outperforms the cyclic detector when the noise power is known perfectly. However, with 1-dB noise uncertainty there is roughly a 5-dB performance gap between the cyclic detector and the energy detector. Moreover, due to the noise uncertainty the performance of the energy detector does not improve if the number of samples increases. This behavior is predicted by the SNR wall [28]. That is, due to the noise uncertainty the energy detector cannot distinguish the weak primary user signal from slightly higher noise power. Consequently, the energy detector is very susceptible to noise uncertainties and thus its performance is dictated by the accuracy of the noise power estimate. This is

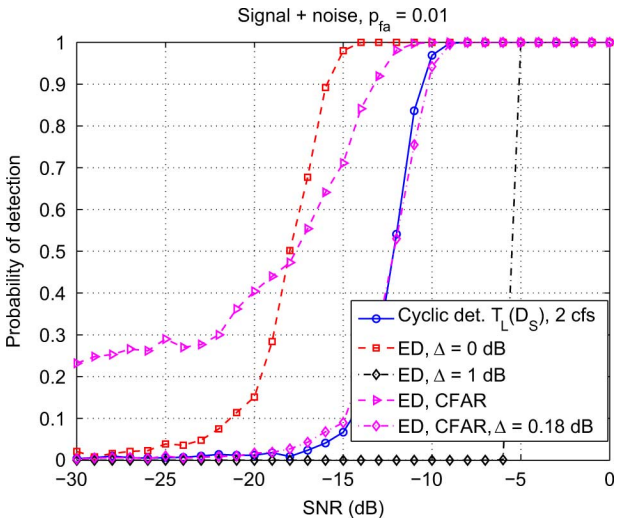

Fig. 4. Probability of detection versus SNR for a WLAN OFDM signal in AWGN. Noise estimation from the guard bands suffers from uncertainty that reduces the reliability of the CFAR energy detector. The noise uncertainty scaled CFAR energy detector has roughly the same performance as the cyclic detector. That is, in this example, the noise uncertainty must be less than 0.18 dB in order to have equal performance to the cyclic detector. Moreover, noise uncertainty makes robust energy detection impossible beyond certain SNR as predicted by the SNR wall. (ED = Energy detector.)

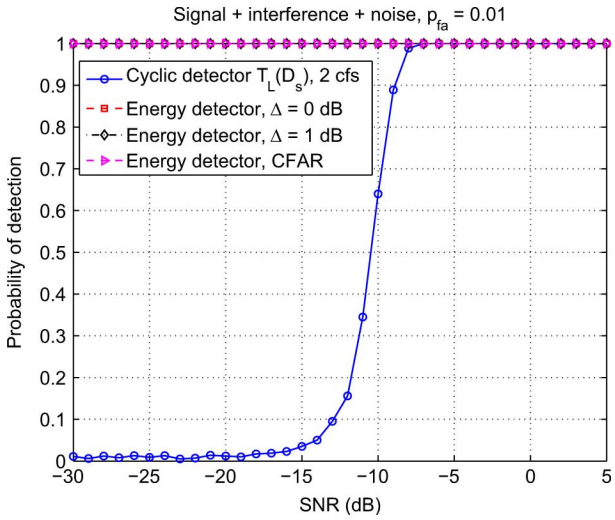

Fig. 5. Probability of detection versus SNR for a WLAN OFDM signal in AWGN. The interfering signal is an OFDM signal with different cyclic frequencies and a narrower bandwidth (1/7th of the primary user signal bandwidth). The SNR of the interfering signal is −5 dB. The energy detector has no means for distinguishing between the primary user signal and the interference. Hence, it will either always detect the presence of the primary user even if only the interfering signal is present or be restricted by the SNR wall depending on the SNR of the interfering signal compared to the noise uncertainty.

demonstrated by the CFAR energy detector. It can be seen that if there is even minor uncertainty in the noise power estimation, the CFAR energy detector cannot limit the false alarm rate reliably or obtain the same detection performance as the energy detector with exactly known noise power. We have experimentally determined from a pure noise signal that the uncertainty in noise power estimation for the false alarm rate 0.01 in this case is roughly 0.18 dB. That is, adding this uncertainty to the estimated noise power results in a false alarm rate of 0.01. Using this uncertainty to scale the noise power estimate the performance of the CFAR energy detector is roughly on the same level with the cyclic detector. This shows that the noise uncertainty must be less than 0.18 dB in this scenario for the CFAR energy detector to obtain the same performance as the cyclic detector. However, this experiment assumes a white noise spectrum without any interference. Practically all communication bands are interference limited in their capacity. In interference limited communication channels it is hard to estimate the noise power reliably. In [29] a 1-dB noise uncertainty is considered to be a typical value without considering interference. If interference is taken into account the noise uncertainty may be significantly higher than 1 dB.

Fig. 5 depicts the performance of the detectors in the presence of one interfering signal. The interfering signal is another OFDM signal ($N_{\mathrm{FFT}} = 32$, $N_{\mathrm{occ}} = 32$, $N_{\mathrm{cp}} = 8$, QPSK) with different cyclic frequencies and a narrower bandwidth (1/7th of the bandwidth of the primary user signal). The SNR of the interference is −5 dB. Since the energy detector is not able to distinguish between the primary user signal and the interference, it will either always detect the presence of the primary user regardless of the SNR of the primary user signal or if the SNR of the interfering signal is low enough compared to the noise uncertainty it will suffer from the SNR wall behavior. The cyclic detector is able to distinguish between the primary user and interfering signals and consequently suffers only a roughly 1–2-dB performance loss compared to the case where interference is not present.

Energy detection has no means of distinguishing among different signals. It is intended for detecting random signals in noise and it does not exploit any knowledge of signal waveforms. In cognitive radio applications we are operating in frequency bands where interference, not just noise, is frequently present. Examples of common interference sources are ultra-wideband devices, other secondary users, device-to-device communication, leakage from adjacent channels as well as electrical devices with electromechanical switches. Cyclostationary detection provides means for distinguishing among primary users, secondary users, and interference.

D. Collaborative Detection With Censoring

Fig. 6 illustrates the performance of the censoring test based on two cyclic frequencies for different communication rate constraints. The test signal is a WLAN OFDM signal with the following parameters: $N_{\mathrm{FFT}} = 64$, $N_{\mathrm{occ}} = 52$, and $N_{\mathrm{cp}} = 16$. The subcarrier modulation is 64-QAM, the signal length is 100 OFDM symbols (= 8000 samples = 0.4 ms), and the channel is a frequency flat Rayleigh fading channel.

It can be seen from the figure that the performance loss due to censoring is minor even under very strict communication rate constraints.

Fig. 7 shows the number of users transmitting their test statistics to the FC as a function of SNR under different communication rate constraints. The reductions in transmissions are largest at low SNRs. At moderate-to-high SNRs more users start to "detect" the presence of the primary user. The value of their local test statistic increases and becomes informative by indicating

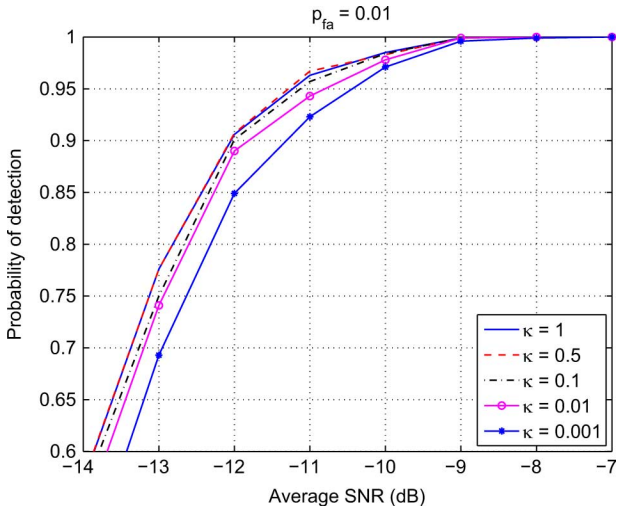

Fig. 6. Probability of detection versus SNR (dB) for a WLAN signal in frequency flat Rayleigh fading channel for different communication rate constraints. The number of collaborating users is 10. The performance with censoring is close to optimal even under very strict communication rate constraints.

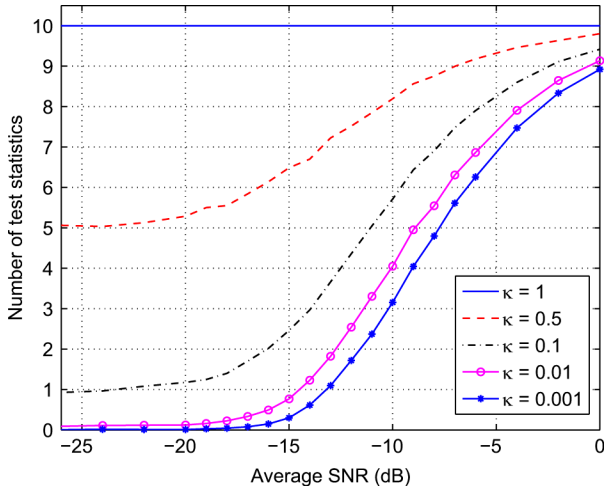

Fig. 7. Average number of users transmitting the test statistic to the FC versus SNR for different communication rate constraints. The number of users transmitting their test statistics to the FC are as imposed by the respective communication rate constraints.

the possible presence of the primary user and consequently they transmit their test statistics to the FC. The very low SNR regime corresponds to the situation when the primary user is not present as well. Hence, we can see that the transmission rates under H_0 are as imposed by the communication rate constraints. Since the null hypothesis situation is the most likely situation in practice, significant savings in overall transmission rates are obtained.

E. Doppler Effect

In this section, the goal is to determine the effects of carrier frequency shifts and the subsequent change in cyclic frequencies due to the Doppler effect on the performance of the cyclic detectors. In order to study these effects, Doppler spread due to the mobility of the receiver (and/or transmitter) is introduced to the channel. In addition, the symbol period is changed proportionally to the maximum Doppler frequency.

Doppler effects are caused by the relative motion of the transmitter and receiver as well as by their relative motion with respect to the reflectors. A sinusoidal transmitted waveform with wavelength λ experiences a frequency shift given by $\Delta f = v/\lambda = v/c \cdot f$ where v is the speed of the transmitter relative to the receiver, c is the speed of the light, and f is the frequency of the sinusoidal waveform. The change in symbol frequencies is proportional to the ratio of the speeds as well, i.e., $\Delta\alpha = v/c \cdot \alpha$. For example, for a DVB-T system in 8-K mode with a cyclic prefix of 1/8 of the useful symbol data, the symbol frequency is approximately 1 kHz. Hence, for a relative speed of 300 m/s the change in symbol frequency is roughly 10^{-3} Hz. In addition, oscillator mismatch between the transmitter and receiver may cause a frequency offset. In practice instead of a single frequency shift the signal experiences a complete Doppler spread. That is, each propagation path experiences a different Doppler shift.

Two test signals are employed: 3GPP LTE (Long term evolution) [30] and DVB-T OFDM signals. The LTE signal parameters are as follows. $N_{\mathrm{FFT}} = 512$, $N_{\mathrm{occ}} = 300$, and $N_{\mathrm{cp}} = 36$. The subcarrier modulation is QPSK, the carrier frequency is 2.5 GHz, and the length of the LTE signal is 14 OFDM symbols (= 7672 samples $\approx$ 1 ms). The DVB-T signal parameters are: $N_{\mathrm{FFT}} = 8192$, $N_{\mathrm{occ}} = 6817$, and $N_{\mathrm{cp}} = 1024$. The subcarrier modulation is 64-QAM, the carrier frequency is 750 MHz, and the length of the DVB-T signal is three OFDM symbols (= 27 648 samples $\approx$ 3 ms). Multicycle sum detectors are employed. The detection is performed at the cyclic frequencies of the original transmitted signal (i.e., without Doppler effect).

Fig. 8 depicts the performance as a function of the SNR for (a) the LTE signal in the 3GPP typical urban multipath channel TUx ($\Delta T = 130.2$ ns) [31] and (b) the DVB-T signal in ETSI EN 300 744 V1.5.1 (2004–11) [32] Rayleigh fading channel for different mobile speeds. The employed Rayleigh fading has the Jakes' Doppler spectrum generated using the model in [33]. It can be seen that the detectors are relatively insensitive to Doppler effects. There is performance loss in the case of the DVB-T signal. However, it is significant only at very high mobile speeds. Such high speeds are not very realistic in practical cognitive radio applications. The DVB-T signal has longer symbol length than the LTE signal, and thus it suffers more from the time selectivity of the channel.

F. Log-Normal Shadowing

In the next simulation, in addition to a Rayleigh fading multipath channel, a log-normal shadowing process is included. The shadowing among secondary users is assumed to be independent.

Fig. 9 illustrates the performance for an LTE signal in the 3GPP typical urban multipath channel TUx ($\Delta T = 130.2$ ns) [31] with a mobile speed of 3 km/h and log-normal shadowing. The log-normal shadowing process has a zero mean and a standard deviation of 6 dB. These parameters have been chosen to model a small-area shadowing process. The signal parameters are as follows. $N_{\mathrm{FFT}} = 512$, $N_{\mathrm{occ}} = 300$, and $N_{\mathrm{cp}} = 36$. The subcarrier modulation is QPSK, and the length of the signal is 14 OFDM symbols (= 7672 samples $\approx$ 1 ms). All the detectors are multicycle sum detectors. All secondary users have equal communication rate constraints.

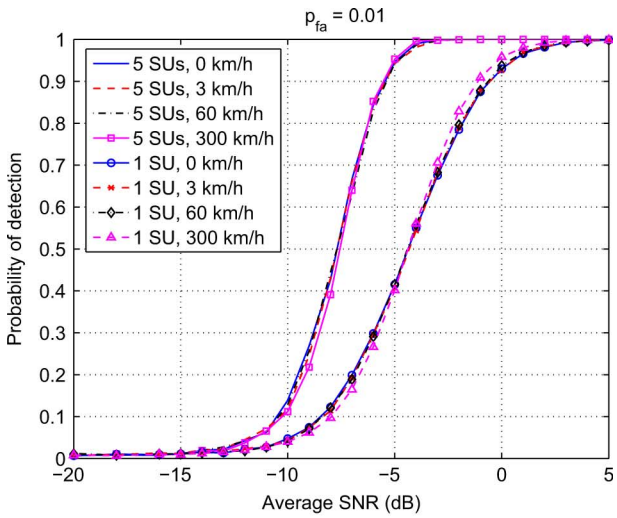

(a) LTE

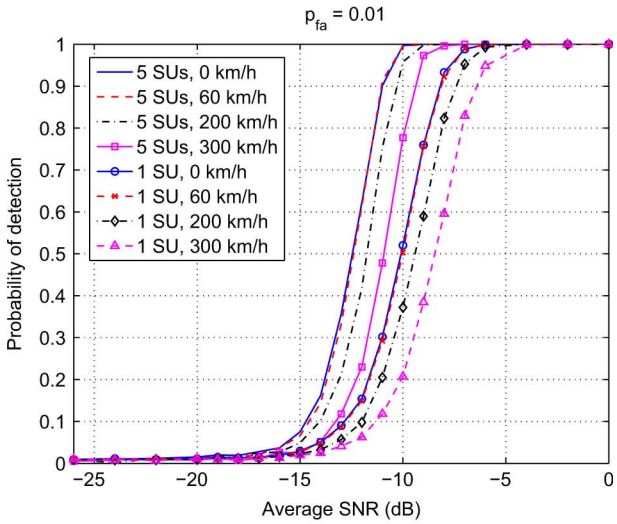

(b) DVB-T

Fig. 8. Probability of detection versus SNR (dB) for (a) an LTE signal in 3GPP Typical Urban Rayleigh fading channel and (b) a DVB-T signal in ETSI EN 300 744 V1.5.1 (2004–11) Rayleigh fading channel for different mobile speeds. The proposed detectors are fairly resistant to Doppler effects.

Fig. 9 shows that shadowing along with fading effects can be effectively mitigated through collaboration among secondary users. Moreover, collaboration is practically a must in order to obtain reliable performance under shadowing and fading effects. In practice, the shadowing processes may be correlated among the secondary users. Thus, the performance gain from collaboration may be reduced as well. Consequently, the importance of spatial diversity among the secondary users is emphasized.

Fig. 9 also shows that censoring works extremely well in shadowed environments compared to the uncensored approach. The performance with strict communication rate constraint $\kappa = 0.01$ is even slightly better in the low SNR regime in this case.

Medium-scale variation of the received signal power is commonly attributed to shadowing. Comparing Fig. 9 to previous figures [especially Fig. 8(a)] one might falsely conclude that shadowing may produce performance gain. However, since shadowing is caused by obstruction of buildings, trees, foliage,

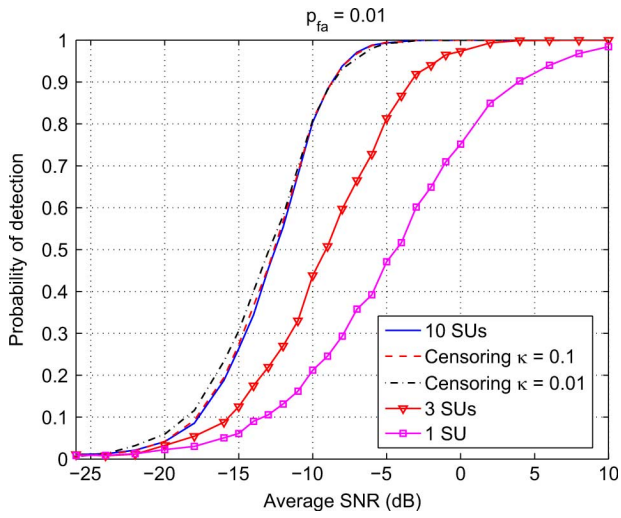

Fig. 9. Probability of detection versus Average SNR (dB) for an LTE signal in a Rayleigh fading channel. Shadowing process has a log-normal distribution with mean of 0 dB and standard deviation of 6 dB. Cooperation among secondary users mitigates loss due to shadowing and multipath.

and other obstacles it cannot be expected to produce any performance gain. Shadowing should be viewed as an additional loss on top of the distance dependent attenuation. Hence, these results should be viewed as showing the performance for a given average receiver SNR where the average SNR depends on the path loss that includes both the distance dependent attenuation as well as the average shadowing loss. The more gentle slope of the performance curves is due to the variation of the received signal power caused by the shadowing process.

VI. Conclusion

In this paper, cyclostationary spectrum sensing of primary users in a cognitive radio system has been considered. We have proposed single user multicycle detectors and extended them to accommodate user collaboration. Moreover, we have proposed a censoring technique for reducing energy consumption and the number of transmissions of local test statistics during collaboration. Unlike energy detection the proposed cyclostationary approach is able to distinguish among primary users, secondary users, and interference. Furthermore, it is not susceptible to noise uncertainty. Moreover, it is nonparametric in the sense that no assumptions on data or noise distributions are required.

Collaboration among secondary users is essential for mitigating the effects of shadowing and fading, and consequently shortening the detection time. However, collaboration generates reporting overhead that increases transmissions by the secondary users. In mobile applications battery life is a limited resource that has to be conserved. A censoring scheme in which only informative test statistics are transmitted to the FC has been proposed. The proposed censoring scheme has been seen as a viable approach for significantly reducing the reporting overhead without sacrificing the performance. Even under very strict constraints on communication rates only a minor performance loss has been observed.

In summary, the proposed method combining cyclostationary detection and user collaboration with censoring provides a powerful energy efficient approach for spectrum sensing in cognitive radio systems.

APPENDIX

In the following the distribution of the maximum of d independent (central) chi-square random variables is derived. It is assumed that the chi-square random variables have $2N_1, 2N_2, \ldots, 2N_d$ degrees of freedom, respectively. The cumulative distribution function of the chi-square distribution with $2N$ degrees of freedom is given by

$$F(x, 2N) = \frac{\gamma\left(N, \frac{x}{2}\right)}{\Gamma(N)} \tag{39}$$

where $\gamma(k, x)$ is the lower incomplete gamma function and $\Gamma(k)$ is the ordinary gamma function. For a positive integer k the following identities hold:

$$\Gamma(k) = (k-1)! \tag{40}$$

$$\gamma(k, x) = \Gamma(k) - (k-1)!\, e^{-x} \sum_{n=0}^{k-1} \frac{x^n}{n!}. \tag{41}$$

Hence, the cumulative distribution function of the chi-square distribution with $2N$ degrees of freedom is given by

$$F(x, 2N) = 1 - e^{-x/2} \sum_{n=0}^{N-1} \frac{\left(\frac{x}{2}\right)^n}{n!}. \tag{42}$$

The cumulative distribution function of the maximum of d independent random variables is the product of the cumulative distribution functions of the individual random variables since

$$\begin{aligned} p(\max_{i=1,\ldots,d} x_i \le a) &= p(x_1 \le a, \ldots, x_d \le a) \\ &= p(x_1 \le a) \cdots p(x_d \le a) \\ &= \prod_{i=1}^{d} p(x_i \le a). \end{aligned}$$

Hence, the cumulative distribution function of the maximum of d (central) chi-square random variables with $2N_1, \ldots, 2N_d$ degrees of freedom respectively is given by

$$F_{\mathcal{D}}(x, d, \{N_i\}_{i=1}^{d}) = \prod_{i=1}^{d} \left(1 - e^{-x/2} \sum_{n=0}^{N_i - 1} \frac{\left(\frac{x}{2}\right)^n}{n!}\right). \tag{43}$$

ACKNOWLEDGMENT

The authors would like to thank Prof. S. A. Kassam from the University of Pennsylvania for very helpful discussions.

REFERENCES

[1] J. Mitola , III and G. Q. Maquire , Jr, "Cognitive radio: Making software radios more personal," *IEEE Pers. Commun.*, vol. 6, no. 4, pp. 13–18, Aug. 1999.

[2] S. Haykin, "Cognitive radio: Brain-empowered wireless communications," *IEEE J. Sel. Areas Commun.*, vol. 23, no. 2, pp. 201–220, Feb. 2005.

[3] I. F. Akyildiz, W.-Y. Lee, M. C. Vuran, and S. Mohanty, "Next generation/dynamic spectrum access/cognitive radio wireless networks: A survey," *Comput. Netw.*, vol. 50, no. 13, pp. 2127–2159, Sep. 2006.

[4] Z. Tian and G. B. Giannakis, "Compressed sensing for wideband cognitive radios," in *Proc. IEEE Int. Conf. Acoustics, Speech, Signal Processing*, Honolulu, HI, Apr. 15–20, 2007, vol. IV, pp. 1357–1360.

[5] A. Ghasemi and E. S. Sousa, "Spectrum sensing in cognitive radio networks: The cooperation-processing tradeoff," *Wireless Commun. Mobile Comput.*, vol. 7, no. 9, pp. 1049–1060, Nov. 2007.

[6] S. M. Mishra, A. Sahai, and R. W. Brodersen, "Cooperative sensing among cognitive radios," presented at the Int. Conf. Communications, Istanbul, Turkey, Jun. 11–15, 2006.

[7] A. V. Dandawaté and G. B. Giannakis, "Statistical tests for presence of cyclostationarity," *IEEE Trans. Signal Process.*, vol. 42, no. 9, pp. 2355–2369, Sep. 1994.

[8] M.Öner and F. Jondral, "Air interface identification for software radio systems," *Int. J. Electron. Commun.*, vol. 61, no. 2, pp. 104–117, Feb. 2007.

[9] J. Wang, T. Chen, and B. Huang, "Cyclo-period estimation for discrete-time cyclo-stationary signals," *IEEE Trans. Signal Process.*, vol. 54, no. 1, pp. 83–94, Jan. 2006.

[10] W. A. Gardner, "Signal interception: A unifying theoretical framework for feature detection," *IEEE Trans. Commun.*, vol. 36, pp. 897–906, Aug. 1988.

[11] L. Izzo, L. Paura, and M. Tanda, "Signal interception in non-Gaussian noise," *IEEE Trans. Commun.*, vol. 40, pp. 1030–1037, Jun. 1992.

[12] W. A. Gardner, A. Napolitano, and L. Paura, "Cyclostationarity: Half a century of research," *Signal Process.*, vol. 86, pp. 639–697, Apr. 2006.

[13] R. Viswanathan and P. K. Varshney, "Distributed detection with multiple sensors: Part I—Fundamentals," *Proc. IEEE*, vol. 85, pp. 54–63, Jan. 1997.

[14] R. S. Blum, S. A. Kassam, and H. V. Poor, "Distributed detection with multiple sensors: Part II—Advanced topics," *Proc. IEEE*, vol. 85, pp. 64–79, Jan. 1997.

[15] G. Ganesan and Y. Li, "Cooperative spectrum sensing in cognitive radio, part I: two user networks," *IEEE Trans. Wireless Commun.*, vol. 6, no. 6, pp. 2204–2213, Jun. 2007.

[16] G. Ganesan and Y. Li, "Cooperative spectrum sensing in cognitive radio, part II: Multiuser networks," *IEEE Trans. Wireless Commun.*, vol. 6, no. 6, pp. 2214–2222, Jun. 2007.

[17] C. R. C. M. da Silva, B. Choi, and K. Kim, "Distributed spectrum sensing for cognitive radio systems," in *Proc. Information Theory Applications Workshop 2007*, La Jolla, CA, Feb. 2, 2007, pp. 120–123.

[18] C. Rago, P. Willett, and Y. Bar-Shalom, "Censoring sensors: A low-communication-rate scheme for distributed detection," *IEEE Trans. Aerosp. Electron. Syst.*, vol. 32, pp. 554–568, Apr. 1996.

[19] S. Appadwedula, V. V. Veeravalli, and D. L. Jones, "Robust and locally- optimum decentralized detection with censoring sensors," in *Proc. 5th Int. Conf. Information Fusion*, Jul. 8–11, 2002, vol. 1, pp. 56–63.

[20] R. S. Blum and B. M. Sadler, "A new approach to energy efficient signal detection," in *Proc. 41st Annu. Conf. Information Sciences Systems (CISS)*, Baltimore, MD, Mar. 14–16, 2007, pp. 208–213.

[21] C. Sun, W. Zhang, and K. B. Letaief, "Cooperative spectrum sensing for cognitive radios under bandwidth constraints," in *Proc. IEEE Int. Wireless Communications Networking Conf. (WCNC 2007)*, Hong Kong, China, Mar. 11–15, 2007, pp. 1–5.

[22] H. E. Rowe, *Signals and Noise in Communication Systems*. London, U.K.: Van Nostrand, 1965.

[23] M. F. Driscoll, "An improved result relating quadratic forms and chi-square distributions," *Amer. Statist.*, vol. 53, no. 3, pp. 273–275, Aug. 1999.

[24] K. Knight, *Mathematical Statistics, Texts in Statistical Science*. Boca Raton, FL: Chapman & Hall/CRC Press, 2000.

[25] J. Gil-Pelaez, "Note on the inversion theorem," *Biometrika*, vol. 38, no. 3/4, pp. 481–482, Dec. 1951.

[26] H. Bohman, "Numerical inversions of characteristic functions," *Scand. Actuarial J.*, pp. 121–124, 1975.

[27] J. Abate and W. Whitt, "The Fourier-series method for inverting transforms of probability distributions," *Queueing Syst.*, vol. 10, no. 1–2, pp. 5–87, Jan. 1992.

[28] R. Tandra and A. Sahai, "SNR walls for signal detection," *IEEE J. Sel. Topics Signal Process.*, vol. 2, no. 1, pp. 4–17, Feb. 2008.

[29] S. Shellhammer and R. Tandra, Performance of the Power Detector with Noise Uncertainty, IEEE Std. 802.22–06/0134r0 Sep. 2, 2008 [Online]. Available: https://mentor.ieee.org/802.22/file/06/22–06-0134–00-0000-performance-of-the-power-detector-with-noise-uncertainty.ppt

[30] 3rd Generation Partnership Project, Technical Specification Group Radio Access Networks, Evolved Universal Terrestrial Radio Access (E-UTRA) and Evolved Universal Terrestrial Radio Access Network (E-UTRAN), Overall description, Stage 2 (Release 8), 3GPP TS 36.300 V8.4.0 Apr. 10, 2008 [Online]. Available: http://www.3gpp.org/ftp/specs/archive/36_series/36.300

[31] 3rd Generation Partnership Project, Technical Specification Group Radio Access Networks, Deployment aspects (Release 7), 3GPP specification: 25.943, 3GPP TR 25.943 V7.0.0 Oct. 1, 2007 [Online]. Available: http://www.3gpp.org/ftp/Specs/html-info/25943.htm

[32] European Telecommunications Standards Institute, Digital Video Broadcasting (DVB), Framing Structure, Channel Coding And Modulation For Digital Terrestrial Television ETSI EN 300 744 v1.5.1 (2004–11), Apr. 10, 2008 [Online]. Available: http://pda.etsi.org/pda/queryform.asp

[33] Y. R. Zheng and C. Xiao, "Improved models for the generation of multiple uncorrelated Rayleigh fading waveforms," *IEEE Commun. Lett.*, vol. 6, pp. 256–258, Jun. 2002.

Jarmo Lundén (S'04) received the M.Sc. (Tech.) degree with distinction in communications engineering from the Department of Electrical and Communications Engineering, Helsinki University of Technology, Espoo, Finland, in 2005, where he is currently working towards the D.Sc. (Tech.) degree.

From September 2007 to March 2008, he was a Visiting Researcher at the University of Pennsylvania, Philadelphia. His research interests include spectrum sensing for cognitive radio as well as radar signal interception and identification.

Visa Koivunen (SM'98) received the D.Sc. (EE) degree (with hons.) from the Department of Electrical Engineering, University of Oulu, Finland.

From 1992 to 1995 he was a Visiting Researcher at the University of Pennsylvania, Philadelphia. From August 1997 to August 1999, he was an Associate Professor at the Signal Processing Laboratory, Tampere University of Technology. Since 1999 he has been a Professor of Signal Processing at the Department of Electrical and Communications Engineering, Helsinki University of Technology (HUT), Finland. He is one of the Principal Investigators in SMARAD (Smart Radios and Wireless Systems) Center of Excellence in Radio and Communications Engineering nominated by the Academy of Finland. He has been also Adjunct Full Professor at the University of Pennsylvania, Philadelphia. During his sabbatical leave in 2006–2007, he was Visiting Fellow at Nokia Research Center as well as visiting fellow at Princeton University. His research interest include statistical, communications, and sensor array signal processing. He has published more than 270 papers in international scientific conferences and journals.

Dr. Koivunen received the primus doctor (best graduate) award among the doctoral graduates in years 1989 to 1994. He coauthored the papers receiving the best paper award in IEEE PIMRC 2005, EUSIPCO 2006, and EuCAP 2006. He has been awarded the IEEE Signal Processing Society Best Paper Award for the year 2007 (coauthored with J. Eriksson). He served as an Associate Editor for the IEEE SIGNAL PROCESSING LETTERS. He is a member of the Editorial Board for the *Signal Processing* journal and the *Journal of Wireless Communication and Networking*. He is also a member of the IEEE Signal Processing for Communication (SPCOM-TC) and Sensor Array and Multichannel (SAM-TC) Technical Committees. He was the General Chair of the IEEE SPAWC (Signal Processing Advances in Wireless Communication) 2007 conference in Helsinki, Finland, in June 2007.

Anu Huttunen was born in Siilinjärvi, Finland, in 1975. She received the M.Sc. degree in engineering physics and mathematics in 1999 and the Doctor of Science degree in electrical and communications engineering from the Helsinki University of Technology, Helsinki, Finland, in 2005.

From 2000 to 2005, she was a Researcher in the Laboratory of Computational Engineering in Helsinki University of Technology. From 2005 to 2008, she was a Research Engineer in Nokia Research Center, Helsinki, Finland. Since 2008, she has been a Senior Design Engineer in Audio Research in Nokia.

H. Vincent Poor (S'72–M'77–SM'82–F'87) received the Ph.D. degree in electrical engineering and computer science (EECS) from Princeton University, Princeton, NJ, in 1977.

From 1977 until 1990, he was on the faculty of the University of Illinois at Urbana-Champaign. Since 1990, he has been on the faculty at Princeton, where he is the Michael Henry Strater University Professor of Electrical Engineering and Dean of the School of Engineering and Applied Science. His research interests are in the areas of stochastic analysis, statistical signal processing, and their applications in wireless networks and related fields. Among his publications in these areas are the recent books *MIMO Wireless Communications* (Cambridge University Press, 2007) and *Quickest Detection* (Cambridge University Press, 2009).

Dr. Poor is a member of the National Academy of Engineering, a Fellow of the American Academy of Arts and Sciences, and a former Guggenheim Fellow. He is also a Fellow of the Institute of Mathematical Statistics, the Optical Society of America, and other organizations. In 1990, he served as President of the IEEE Information Theory Society, and in 2004–2007 he served as the Editor-in-Chief of the IEEE TRANSACTIONS ON INFORMATION THEORY. He was the recipient of the 2005 IEEE Education Medal. Recent recognition of his work includes the 2007 IEEE Marconi Prize Paper Award, the 2007 Technical Achievement Award of the IEEE Signal Processing Society, and the 2008 Aaron D. Wyner Award of the IEEE Information Theory Society.